remote sensing

MDPI

Article

Habitat Classification Predictions on an Undeveloped Barrier Island Using a GIS-Based Landscape Modeling Approach

Emily R. Russ [1,*], Bianca R. Charbonneau [1], Safra Altman [1], Molly K. Reif [1] and Todd M. Swannack [1,2]

[1] US Army Engineer Research and Development Center, Vicksburg, MS 39180, USA; bianca.m.charbonneau@usace.army.mil (B.R.C.); safra.altman@usace.army.mil (S.A.); molly.k.reif@usace.army.mil (M.K.R.); todd.m.swannack@usace.army.mil (T.M.S.)
[2] Department of Biology, Texas State University, San Marcos, TX 78666, USA
* Correspondence: emily.r.russ@usace.army.mil

Abstract: Landscape models are essential tools that link landscape patterns to ecological processes. Barrier island vegetation communities are strongly correlated with geomorphology, which makes elevation-based metrics suitable for developing a predictive habitat classification model in these systems. In this study, multinomial logistic regression is used to predict herbaceous, sparse, and woody habitat distributions on the North End of Assateague Island from slope, distance to shore, and elevation change, all of which are derived from digital elevation models (DEMs). Sparse habitats, which were generally found closest to shore in areas that are exposed to harsh conditions, had the highest predictive accuracy. Herbaceous and woody habitats occupied more protected inland settings and had lower predictive accuracies. A majority of woody cells were misclassified as herbaceous likely because of the similarity in the predictive parameter distributions. This relatively simple model is transparent and does not rely on subjective interpretations. This makes it an effective tool that can directly aid practitioners making coastal management decisions surrounding storm response planning and conservation management. The model results were used in a nutrient sequestration application to quantify carbon and nitrogen stored in barrier island vegetation. This represents an example of how the model results can be used to assign economic value of ecosystem services in a coastal system to justify different management and conservation initiatives.

Keywords: ecological model; digital elevation model; habitat classification; multinomial logistic regression; nutrient sequestration; coastal management

Citation: Russ, E.R.; Charbonneau, B.R.; Altman, S.; Reif, M.K.; Swannack, T.M. Habitat Classification Predictions on an Undeveloped Barrier Island Using a GIS-Based Landscape Modeling Approach. *Remote Sens.* **2022**, *14*, 1377. https://doi.org/10.3390/rs14061377

Academic Editors: Valeria Tomaselli, Maria Adamo and Cristina Tarantino

Received: 25 January 2022
Accepted: 9 March 2022
Published: 12 March 2022

1. Introduction

Coastal zone habitats such as salt marsh, maritime forest, and dunes provide a variety of ecosystem services including flood protection for habitats and infrastructure, recreational opportunities, resources, and habitat space [1]. Understanding the cause and effects of their changing distributions is a topic of growing concern given that coastal habitats are globally threatened by climate change and anthropogenic pressure [2–6]. Barrier island systems support a variety of these coastal zone habitats and provide a protective buffer to inland bay, estuarine, and wetland environments. As the first line of defense to mainland coastal shorelines, barrier islands are particularly sensitive to physical stressors such as sea level rise and storm disturbances.

Geomorphic and biological patterns and processes on barrier islands are inextricably linked such that topography dictates species or habitat distributions, and species distributions in turn affect landscape change [7,8]. Landscape ecology has historically focused on connecting spatial patterns with ecological processes to predict or model vegetation distributions [9,10]. Towards this goal, landscape metrics, derived from in situ and remotely sensed data, have been related to coastal habitat gradients and can therefore be used for predicting species distributions (e.g., [11,12]). For example, local topographic variation can

represent signatures of different species, which have been used to define distributions in ecogeomorphic habitats [13–15]. Spatially predictable abiotic stressors are highly correlated with habitat and species distributions, which enables identification of habitat or species distribution thresholds from stress gradients extracted from elevation data [13,16].

Elevation and distance to shore are the most common landscape metrics linked to barrier island vegetation habitats. These metrics are physical proxies to many abiotic stressors controlling vegetation distribution on barrier islands [16–20]. For example, distance to shore can represent salinity and/or disturbance exposure, where vegetation closer to shore must be adapted to harsher conditions (e.g., higher salinities and burial), while more salt-sensitive species are found farther inland. Elevation is often used to indicate water stress and flooding vulnerability, with water stress-tolerant species found on dunes and flood-tolerant species in marshes [17,18].

Remote sensing data, such as lidar and satellite/aerial imagery, can be important resources to monitor coastal dynamics at high spatial and temporal resolutions over larger spatial extents than can be covered through field-based efforts. Lidar data have been used in numerous studies to develop digital elevation models (DEMs) that are then analyzed to capture geomorphic features and changes shaped by various coastal processes [21]. These elevation map products can inform coastal management decisions related to sediment transport, sea level rise, and storm impacts [22,23]. Similarly, satellite and aerial imagery has been widely used in coastal areas to identify habitat boundaries (e.g., wetland extent) by implementing supervised and unsupervised classification algorithms, and track changes in coverage, which can be used to inform conservation strategies, especially in vulnerable areas (e.g., [24]). Several studies have also demonstrated that coastal habitat classification accuracy can further be refined by integrating multiple remote sensing datasets (i.e., lidar, imagery, and field-based observations) to provide highly accurate and detailed products for coastal zone management [25,26].

Although vegetation data exist in some areas, they are usually collected less routinely than elevation data and often over smaller spatial extents [27,28]. Additionally, using high-resolution, multispectral aerial imagery to delineate vegetation habitats is more computationally expensive, with larger file sizes and more processing steps that require specialized knowledge, than using single-band elevation data at comparable resolutions. Therefore, using publicly available elevation data to predict coastal vegetation habitats can potentially overcome scale (spatial and temporal) and processing limitations to make habitat data more accessible for coastal managers. The purpose of this study is to (1) develop a model that uses elevation-based landscape metrics, which are linked to ecological processes, to classify vegetation habitats using Assateague Island as a case study; (2) determine the accuracy of the predictions by habitat type; and (3) calculate nutrient (C, N) sequestration from the model results to demonstrate the first step for quantifying ecosystem service value. Using landscape metrics to classify habitat and, in turn, organic matter accumulation allows for greater insight on how habitat change may affect rapid carbon sequestration, a process that has not been widely studied in barrier island systems [29]. Understanding potential C and N sequestration in barrier islands highlights their role in global C and N budgets and also serves as a modeled example of integrating landscape-level measures to ecosystem processes. By rapidly assessing landscape classes from readily and publicly available elevation data, this model is made accessible to managers and practitioners, linking critical ecological processes to landscape planning and operations [4,5].

2. Study Area

Assateague Island is a largely undeveloped, microtidal, and wave-dominated barrier island complex that spans 60 km along the Maryland and Virginia coasts. This study focuses on the northernmost 10 km (hereafter referred to as the North End), which includes ~4.5 km^2 of the Assateague Island National Seashore (ASIS) managed by the National Park Service (NPS). It is bound by Ocean City Inlet, Assateague State Park, the Atlantic Ocean, and Sinepuxent Bay to the north, south, east, and west, respectively (Figure 1). The

highly dynamic North End is relatively low-lying, narrow, and erosive due to frequent storm impacts and sediment deficits caused by the Ocean City Inlet jetties constructed in 1935 to stabilize the Inlet for navigation [30]. The prolonged sediment loss prompted emergency management actions, including construction of a low-elevation foredune to prevent breaching and a long-term restoration project to mitigate erosion and to protect island integrity [30–32].

The North End is made up of predominately unvegetated beach, sparsely vegetated dunes, fringing salt marsh, and forest and shrub habitats [28,33]. Vegetation patterns on the North End are strongly correlated with geomorphology, such that dune vegetation is sparse and largely overwash driven while shrubs, maritime forests, and salt marshes have developed inland of the sheltering foredune [34]. The North End supports a variety of threatened and endangered species, such as the *Amaranthus pumilus* (seabeach amaranth) and *Charadrius melodus* (piping plover). Sparsely vegetated overwash areas are critical nesting habitats for piping plover, which are monitored annually by the NPS to measure breeding success [30].

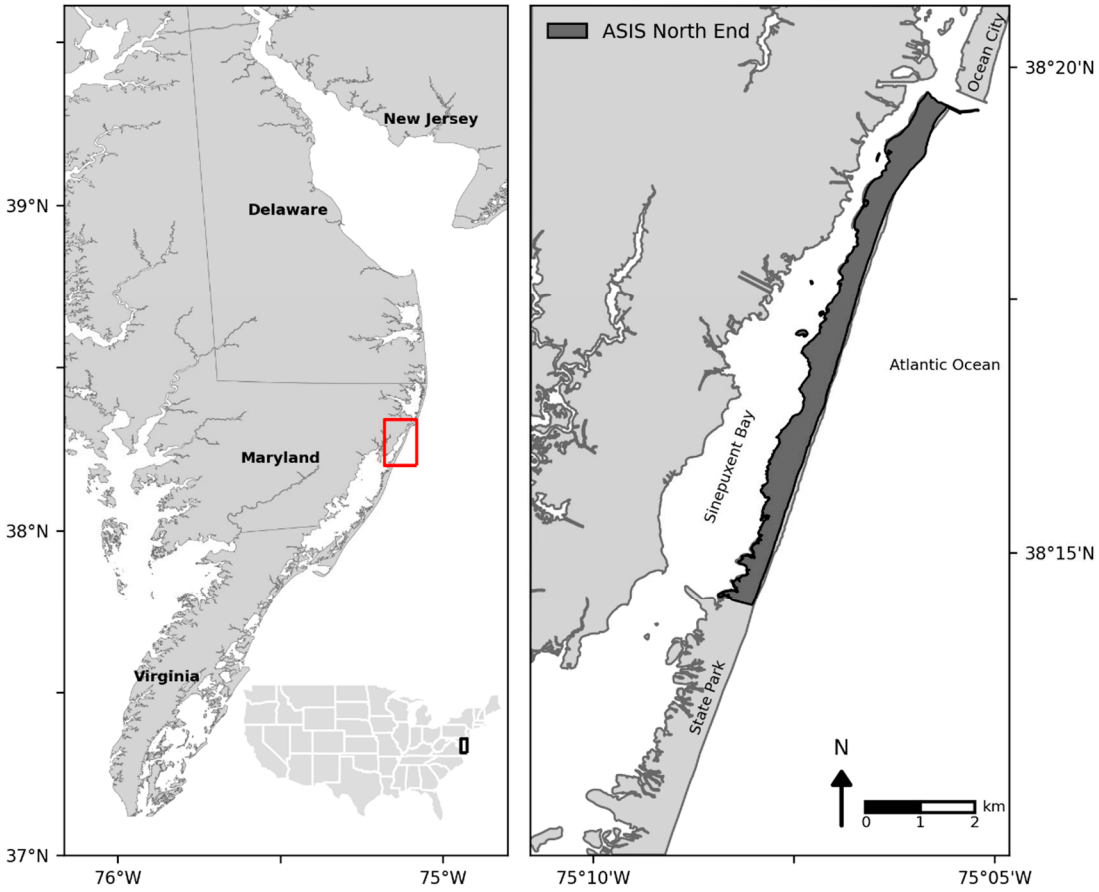

Figure 1. Site map of North End of Assateague Island (ASIS), shown in dark gray.

3. Materials and Methods

3.1. Geospatial Data and Processing

There is a wealth of publicly available, high-resolution and multitemporal remote sensing data for the North End that were utilized for the landscape analysis. The NPS mapped North End vegetation habitats from aerial imagery and field surveys between 1994 and 2012 as part of an effort to monitor piping plover breeding activities. Habitats were defined by vegetation coverage and classified as sparse (<20% vegetative cover, including bare), herbaceous (wetland and upland covering at least a 25 m^2 area at >20% cover), or woody (recognizable stand of shrubs or trees). Lidar data have been collected along the

East Coast by a variety of Federal agencies for mapping shoreline change and are listed in Table 1. For this study, piping plover habitat data with 1 m horizontal accuracy (2012) were obtained from the NPS ASIS data repository (https://asis-nps.opendata.arcgis.com/; accessed on 1 June 2021). DEMs derived from lidar data (2000 and 2012) were obtained from NOAA's Digital Coast; Table 1 includes horizontal and vertical accuracies associated with the lidar data. The DEMs were clipped to the extent of the habitat data and resampled to 5 m resolution using nearest-neighbor interpolation. The 5 m spatial resolution was chosen as a common resolution that also optimized computation time and power.

Table 1. Lidar data specifications (year, cell size, vertical and horizontal accuracy, agency, and sensor) for ASIS 2000 [35] and 2012 [36].

Year	Cell Size (m)	Vertical Accuracy (cm)	Horizontal Accuracy (cm)	Agency	Sensor
2000	3	15	80	NOAA, NASA, USGS	Airborne Topographic Mapper
2012 *	1	7	30	USACE	Optech Gemini Lidar Sensor

* Post Hurricane Sandy.

Six DEM-derived metrics linked to barrier island vegetation growth and distribution patterns (Figure 2) were identified from a database that relates ecological processes to landscape patterns and metrics [4]. Elevation change (between two DEMs), slope, and distance to shore (distance to zero contour; Figure 2) were selected for inclusion in the habitat model after removing highly correlated metrics. The Geospatial Data Abstraction Library (GDAL) tools gdaldem, gdal_proximity.py, and gdal_calc.py were used to develop surfaces of the three selected metrics. The habitat data were downloaded in vector format and then rasterized to the same extent and cell size as the DEM-derived parameters. Each raster was then converted from a 2D array to an XYZ dataset and merged into a single dataset by XY coordinates. Any rows with missing data were removed. A cube-root transformation was applied to the slope and distance-to-shore values to normalize their distribution.

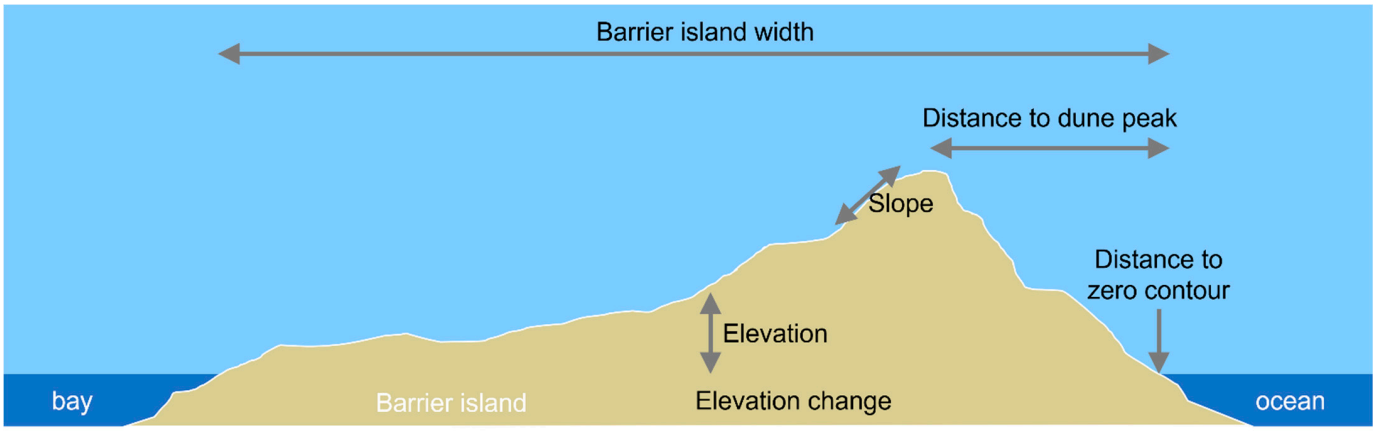

Figure 2. Six parameters that are derived from a DEM that influence vegetation growth and distribution on a barrier island.

3.2. Model Development

Multinomial logistic regression is a statistical approach that uses probabilities to predict categorical data (>2 categories) from a set of independent variables. Multinomial logistic regression was performed in Python 3.8 (using scikit-learn 0.24.1) [37] to develop a model classifying herbaceous, sparse, and woody habitats from the following DEM-derived metrics: elevation change, transformed slope, transformed distance to shore, and product

of transformed slope and distance to shore. The logarithm of the probability of habitat k is represented by the following log-linear equation:

$$\ln(\Pr(Y_i = k)) = \beta_k \cdot X_i - \ln(Z) \quad (1)$$

where β_k is a vector of length m, the number of explanatory variables, of regression coefficients associated with classification k; X_i, also length m, is a vector of the explanatory variables at observation i; and $\ln(Z)$, the intercept. Z is a partitioning value to ensure the probabilities of all habitats (k) sum to one:

$$Z = \sum_{k=1}^{K} e^{\beta_k \cdot X_i} \quad (2)$$

Note, β_k and $\ln(Z)$ are unique for each classification, and thus 3 separate equations were developed to predict the probability of herbaceous, sparse, and woody habitats at each grid cell. Because the probabilities of each habitat must sum to one, the probability of habitat c is described by:

$$\Pr(Y_i = c) = \frac{e^{\beta_c \cdot X_i}}{\sum_{k=1}^{K} e^{\beta_k \cdot X_i}} \quad (3)$$

This is the general form of the probability equation in which the numerator accounts for exponentiating the first term of Equation (1) (a single habitat, c) and the denominator is calculated by exponentiating $\ln(Z)$, Equations (1) and (3) were developed from the whole dataset (DEM-derived metrics as inputs and habitat classifications as output). These equations were then used to calculate habitat classification probabilities and the predicted output was the habitat with the maximum probability. The 2000 DEM was only used to calculate elevation change (2012–2000), while the 2012 DEM was used to calculate slope and distance to shore. The 2012 habitat classification raster was compared to the model output to assess overall model accuracy, producer and user accuracy, and the kappa statistic [38,39].

A nutrient sequestration application was explored to estimate how much carbon and nitrogen are sequestered annually in herbaceous and woody barrier island vegetation using elevation and vegetation habitat data collected on Assateague Island (Table 2) [40]. The elevation ranges reflect the topographic zones in which different herbaceous and woody communities were found. The sequestration rates, aggregated into the elevation ranges, were determined from herbaceous biomass, leaf, and wood litter measurements. Nutrient sequestration rates were assigned to each grid cell and multiplied by 25 to account for grid cell area, using the 2012 elevation and observed and modeled vegetation results. Nutrient sequestration in sparse habitats was assumed to be zero. Nutrient concentrations above 1.41 and 1.20 m elevation in herbaceous and woody habitats, respectively, were not measured and were assigned the average values for herbaceous and forest communities [40].

Table 2. Nutrient (carbon and nitrogen) sequestration rates based on habitat type and elevation [40].

Habitat	Elevation Range (m)	Carbon Sequestration (g C m^{-2} y^{-1})	Nitrogen Sequestration (g N m^{-2} y^{-1})
Herbaceous	0.00–0.66	181.04 ± 15.74	3.52 ± 0.33
	0.67–1.04	171.25 ± 30.67	3.68 ± 0.72
	1.05–1.41	65.28 ± 11.97	1.36 ± 0.27
	>1.41	112.00 ± 14.00	2.24 ± 0.28
Woody	−0.02–0.38	447.29 ± 56.09	6.65 ± 0.93
	0.39–0.79	553.90 ± 87.97	8.70 ± 1.59
	0.80–1.20	531.97 ± 41.88	6.14 ± 0.76
	>1.20	497.00 ± 43.00	5.58 ± 0.48

4. Results

In 2012, the North End was made up of 37%, 45%, and 18% herbaceous, sparse, and woody habitats, respectively (see Figure 3A). Frequency (normalized to habitat cell count)

distributions of the transformed DEM-derived parameters are shown in Figure 4. Summary statistics (minimum, maximum, mean, and standard deviation) corresponding to Figure 4 are listed in Table 3. Although generally similar across habitats, elevation difference varies slightly more in sparse habitats (from −4.22 to 2.90 m; average 0.17 ± 0.57 m) relative to herbaceous (from −2.66 to 3.09; average 0.23 ± 0.39 m) and woody (from −5.89 to 2.83; average −0.04 ± 0.60), as evidenced by the shorter and broader distribution and large standard deviation (Figure 4A). The standard deviation of elevation difference in woody habitat is slightly larger than sparse because of the influence of extreme values (i.e., the long tail) despite having an overall narrower distribution. Slope summary statistics (values are expressed as cube root of % slope) are similar for the three habitats but, unlike herbaceous (from 0.00 to 2.64; average 0.99 ± 0.36) and woody (from 0.00 to 2.81; average 1.04 ± 0.31), sparse habitats display a bimodal distribution (from 0 to 2.68; average 0.95 ± 0.30), with relative maximums at 0.74 and 1.18 (Figure 4B). Differences between habitats are most apparent in the distance-to-shore parameter, in which values are expressed as cube root of distance in meters. Herbaceous (from 3.56 to 8.68; 6.54 ± 0.91) and woody habitats (from 4.57 to 8.16; average 6.79 ± 1.31) both show a relatively normal distribution, with woody habitats occurring over a narrower range. Sparse habitats, which range from 0 to 8.60 (average 4.91 ± 1.31) are generally found closest to the shore, but are also present, albeit less frequently, on the bay side of the barrier island (Figure 4C).

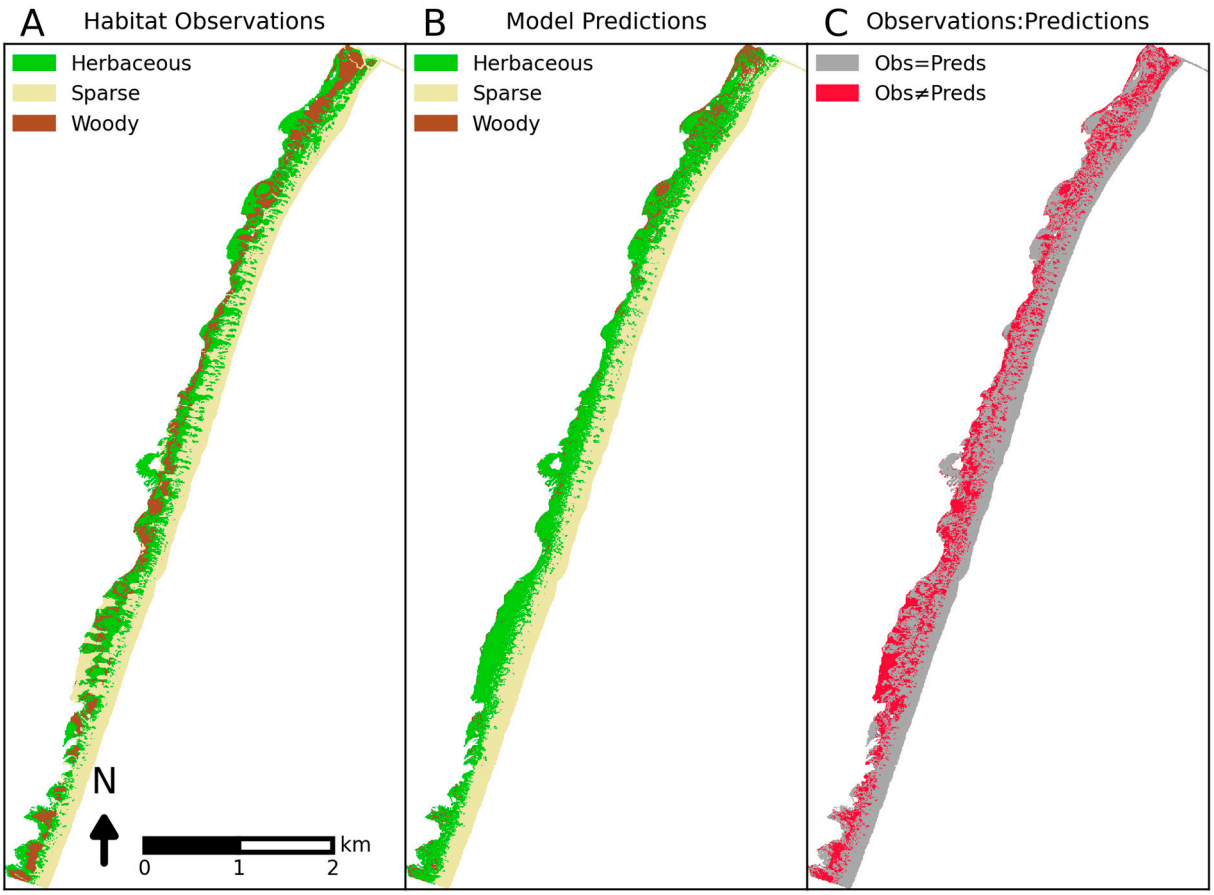

Figure 3. The 2012 habitat observations (**A**), habitat predictions using the equations from Table 4 (**B**), and model accuracy assessment (**C**) in which observations were compared to predictions.

Table 3. Raster summary statistics (minimum, maximum, mean, and standard deviation), grouped by habitat, of the transformed DEM-derived metrics. The * means\times.

Parameter	Minimum	Maximum	Mean	Std. Dev
All (n = 161,346)				
Elevation difference (m)	−5.89	3.09	0.15	0.53
[Slope (%)]$^{1/3}$	0.00	2.81	0.98	0.33
[Distance to shore (m)]$^{1/3}$	0.00	8.68	5.84	1.37
[Slope*Distance to shore]$^{1/3}$	0.00	21.14	5.62	2.08
Herbaceous (n = 58,913)				
Elevation difference (m)	−2.66	3.09	0.23	0.39
[Slope (%)]$^{1/3}$	0.00	2.64	0.99	0.36
[Distance to shore (m)]$^{1/3}$	3.56	8.68	6.54	0.91
[Slope*Distance to shore]$^{1/3}$	0.00	18.85	6.33	1.98
Sparse (n = 73,382)				
Elevation difference (m)	−4.22	2.90	0.17	0.57
[Slope (%)]$^{1/3}$	0.00	2.68	0.95	0.30
[Distance to shore (m)]$^{1/3}$	0.00	8.60	4.91	1.31
[Slope*Distance to shore]$^{1/3}$	0.0	19.93	4.50	1.55
Woody (n = 29,051)				
Elevation difference (m)	−5.89	2.83	−0.04	0.60
[Slope (%)]$^{1/3}$	0.00	2.81	1.04	0.31
[Distance to shore (m)]$^{1/3}$	4.57	8.16	6.79	1.31
[Slope*Distance to shore]$^{1/3}$	0.00	21.14	6.99	2.00

Table 4 lists the values of β_k (4 regression coefficients that correspond to each explanatory variable: elevation difference, slope, distance to shore, and slope times distance to shore) and ln(Z) (intercept) for the log-linear equations (Equation (1)) that were developed for each habitat using multinomial logistic regression. Probabilities for each habitat type at each grid cell (X_i) were calculated by exponentiating the log-linear equations into the form of Equation (3), and the habitat with the maximum probability was selected as the model output (Figure 3B).

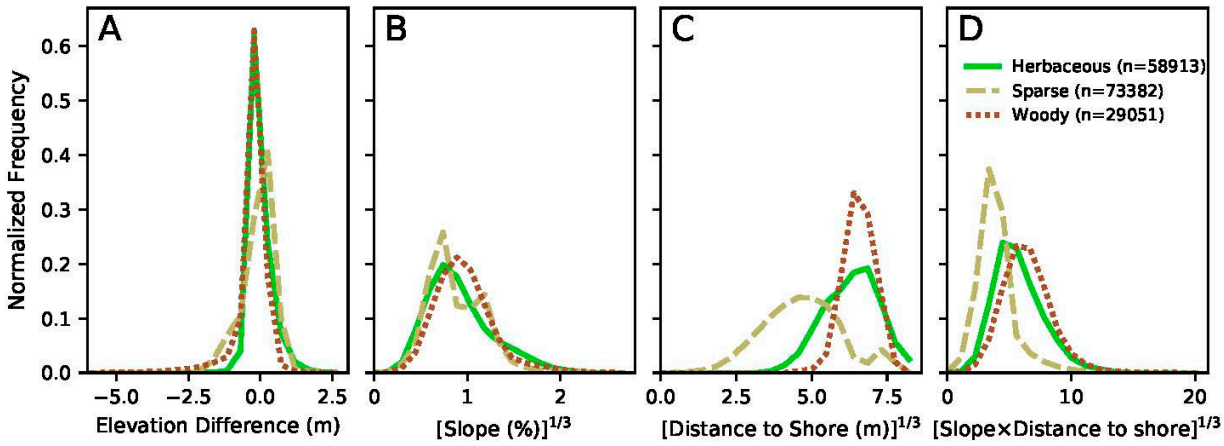

Figure 4. Frequency distributions, normalized by the sum of cells per habitat, of the transformed DEM-derived parameters ((**A**) = elevation difference, (**B**) = Slope, (**C**) = distance to shore, (**D**) = slope × distance to shore).

Table 4. Log-linear equation intercepts and regression coefficients developed to predict probability of 2012 herbaceous, sparse, and woody habitat types from 2012 and 2000 DEM-derived metrics.

	Intercept	Elevation Difference	Slope$^{(1/3)}$	Distance to Shore$^{(1/3)}$	(Slope × Distance to Shore)$^{(1/3)}$
Herbaceous	−6.56	−0.63	3.87	0.98	−0.50
Sparse	7.82	0.08	−0.03	−0.94	−0.32
Woody	−1.26	−0.71	−3.84	−0.03	0.82

An error matrix comparing number of cells per habitat between observations and predictions is shown in Table 5 to evaluate model performance. Overall, 67.6% of the cells were classified correctly (the diagonal in the matrix). Producer accuracy was 82.2%, 72.9%, and 20.1% and user accuracy was 81.7%, 56.1%, and 53.5% for sparse, herbaceous, and woody habitats, respectively. Differences between producer and user accuracies in herbaceous and woody habitats largely reflect woody habitats that were misclassified as herbaceous (Table 4) as the model over-predicted herbaceous habitat area by 30.1% and under-predicted woody habitat area by 62.4%. The model has a kappa statistic of 0.47, indicating moderate agreement between the observations and model predictions [41].

The spatial distributions of habitat agreements and confusions (i.e., comparing grid cells between observations in Figure 3A and model classification in Figure 3B) are shown in Figure 3C. For more detail, see Figure S1, which illustrates the spatial distribution of the six possible habitat confusions. Since the habitat requirement distributions dictated by the DEM-derived metrics are similar for herbaceous and woody habitats (see Figure 4), the confusions between these habitats were assumed more likely than confusion between sparse and woody habitats. Only 6% of herbaceous habitat was misclassified as woody habitat, predominately in the northernmost 1 km, while 75% of woody habitats were misclassified as herbaceous and distributed along the total length of the North End. Approximately 20% of herbaceous habitat was misclassified as sparse, and instances of this were typically closer to the shore, whereas the 16% of sparse habitat that was misclassified as herbaceous was found closer to the Bay shore. There was relatively less confusion (<5%) between woody and sparse habitats.

Table 5. Error matrix with observations along the rows and predictions along the columns. The sum of the rows represents the habitat observations, while the sum of the columns represents the model predictions.

		Predictions			
	Habitat	**Herbaceous**	**Sparse**	**Woody**	**Total**
Observations	Herbaceous	42,976	11,944	3993	58,913
	Sparse	12,000	60,291	1091	73,382
	Woody	21,656	1550	5845	29,051
	Total	76,632	73,785	10,929	161,346

Maximum probabilities of the correct and incorrect classifications are shown in Figure 5 to evaluate model prediction confidence. The average maximum probability of the correctly classified cells (n = 109,112) was 0.58 ± 0.09, 0.85 ± 0.15, and 0.62 ± 0.15 for herbaceous, sparse, and woody habitats, respectively. A majority of these classifications (80% herbaceous, 96% sparse, and 79% woody) had a maximum probability that was greater than the sum of the probabilities of the other two habitat types, ranging from 0.50 to 1.00. Of the incorrectly classified cells (n = 52,234), the average maximum probability was 0.60 ± 0.13, 0.58 ± 0.10, and 0.55 ± 0.08 for herbaceous, sparse, and woody habitats, respectively. Similarly to the correct classifications, 76% herbaceous, 77% sparse, and 76% woody habitat misclassifications had a maximum probability that was greater than the sum of the probabilities of the other two habitats, indicating that misclassifications were not due to relatively low maximum probabilities. Instead, the incorrect classifications were

likely because the cell DEM-derived parameters were more representative of the incorrect habitat than the correct habitat. Most of the incorrectly classified woody habitat cells were classified as herbaceous (Table 4) and were more similar to the herbaceous cells (Figure 6).

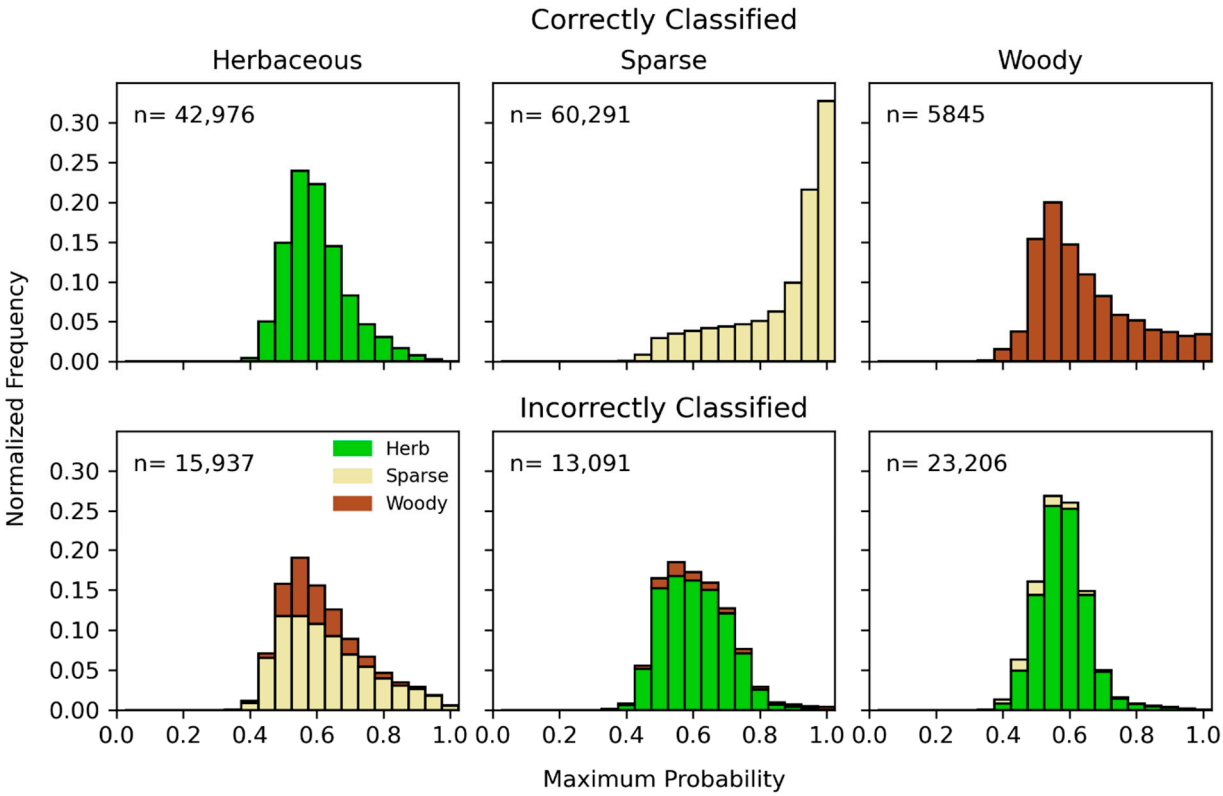

Figure 5. Distribution of maximum probabilities of correctly classified cells (**top row**) and incorrectly classified cells (**bottom row**) by habitat (columns).

Carbon and nitrogen sequestration on the North End was calculated for each grid cell using elevation and habitat data (see Table 2). Values were calculated using habitat observations (Figure 7A,B) and habitat model predictions (Figure 7C,D). Total carbon sequestration based on the habitat observations ranged from 516.16 to 656.31 t C m^{-2} y^{-1}, with 36% from herbaceous vegetation and 64% from woody vegetation. Similarly, nitrogen sequestration based on observations ranged from 7.17 to 9.50 t N m^{-2} y^{-1}, with 38% and 62% attributed to herbaceous and woody vegetation, respectively. Total carbon and nitrogen sequestration based on habitat model predictions ranged from 374.95 to 473.08 t C m^{-2} y^{-1} (68% herbaceous and 32% woody) and from 5.87 to 7.62 t N m^{-2} y^{-1} (73% herbaceous and 27% woody), respectively. Although the calculated nutrient sequestration values are similar for both the observations and model predictions, the contributions from herbaceous and woody vegetation are flipped.

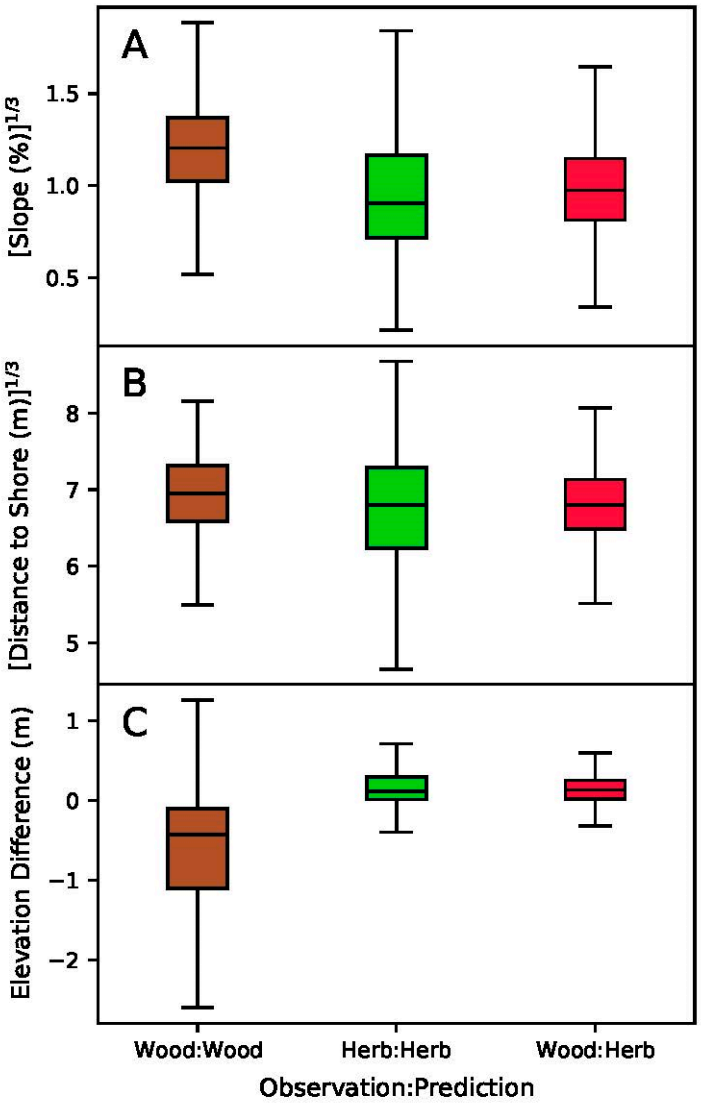

Figure 6. Box plots of (**A**) transformed slope, (**B**) transformed distance to shore, and (**C**) elevation difference of correctly identified woody habitats (left), correctly identified herbaceous habitats (center), and woody habitats that were incorrectly identified as herbaceous habitats (right).

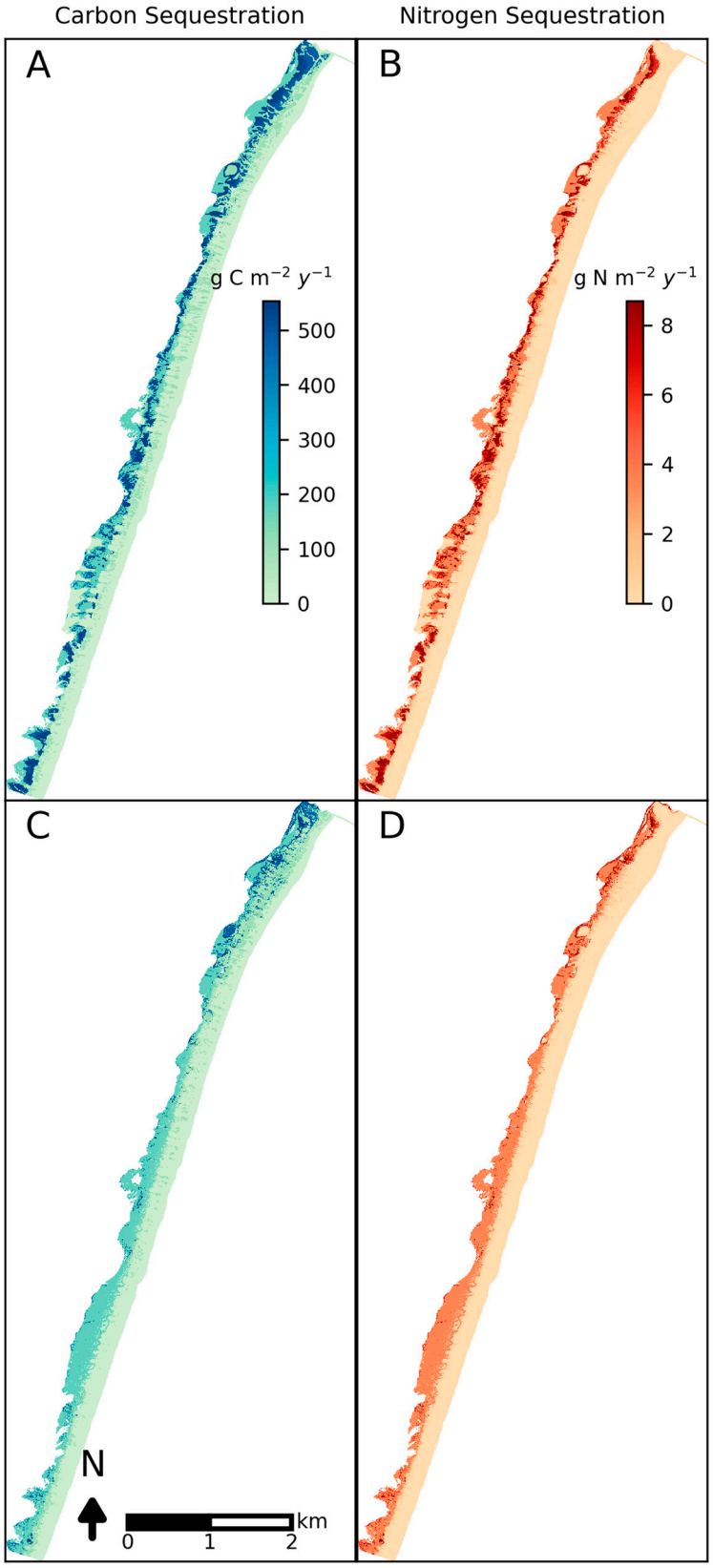

Figure 7. Calculated nutrient sequestration using 2012 DEM and habitat observations for (**A**) carbon and (**B**) nitrogen and using 2012 DEM and habitat model predictions for (**C**) carbon and (**D**) nitrogen.

5. Discussion

Because barrier islands encompass a range of habitats that provide different ecosystem services, which are growing increasingly vulnerable to climate change, it is imperative to classify habitat types at the system level to better understand and quantify barrier island resilience [42]. Vegetation plays a critical role in barrier island stability, from enhancing dune recovery following an overwash event [43] to attenuating wave and current energy and facilitating sediment deposition in marshes [44]. Although woody habitat can help stabilize barrier islands, it is more resistant to rapid geomorphic change than herbaceous vegetation, and woody habitat expansion may reduce long-term barrier island resilience [45]. Identifying transitions between habitat zones can inform habitat use across a barrier island [46] as well as storm response and recovery [47].

The model is most well suited for classifying sparse and herbaceous habitats, with the greatest accuracy surrounding sparse vegetation, suggesting that the DEM-derived metrics are appropriate proxies for the ecological processes controlling their distribution on the North End. Similar to conclusions presented in Ziegler et al. [46], the physical proxies do a good job of differentiating seaward-facing sparse habitats from those of more moderate coverage densities found farther inland. The confusions between sparse and herbaceous habitats in this example largely stemmed from herbaceous habitats found closer to shore or sparse habitats closer to the bay than might be expected [17]. The relatively high accuracy for sparse classifications is likely due to the inclusion of bare cells, which is expected to be a large portion of the sparse habitat since oceanward plants maintain strict limits regarding distance to shoreline for establishment and survival [16,18]. It may be beneficial to distinguish between beach habitat unsuitable for plant growth and sparsely vegetated backshore and dune. This distinction would be helpful for managers working to predict potential future storm response, which is affected by beach width relative to storm surge and planning planting efforts to establish setback limits [48].

Conversely, the model misclassified a majority of woody cells as herbaceous. These errors primarily occurred because there was little difference between the herbaceous and woody habitat requirements reflected in the parameter distributions (Figure 4). Although the overall accuracy was comparable to other elevation-based modeling studies on barrier islands [20,46,49], woody vegetation classification could be improved by including additional parameters that can better distinguish between woody and herbaceous vegetation, such as access to freshwater lens [50,51] or soil age [52]. However, woody species, such as *Morella* sps., may exhibit more plasticity than the literature suggests, warranting further investigation into their ranges to improve habitat classification efforts surrounding them [18]. Vegetation height information, which can be acquired from the first return of lidar data, would help distinguish between woody and herbaceous vegetation, but requires additional processing of raw lidar point clouds [53].

Differences in data collection methods (i.e., subjective interpretation of aerial imagery and field surveys versus elevations derived from remote sensing) and survey timing mismatch (i.e., habitat data collected pre-Hurricane Sandy and elevation data collected post-Hurricane Sandy) could cause errors in the relationships between landscape patterns and ecological processes. Although the habitat data are assumed to be "correct", it may in fact have errors from the manual delineation process, which could skew the relationships between landscape metrics and habitat type [54]. More accurate habitat classifications, such as those derived from the Field spectral libraries, airborne Hyperspectral imagery, and Lidar altimetry (FHyL) method may better align the habitat and geomorphic data and reveal additional predictive metrics, but this is more involved than a DEM-based approach [26].

One of the main strengths of the model is that it is a relatively simple, but effective tool that integrates readily available and routinely collected lidar elevation data, statistics, and modeling techniques to predict habitat distributions on a barrier island. Classification using multinomial logistic regression is more transparent and understandable (i.e., user friendly) than other machine learning algorithms (e.g., [20]). It does not require prior system

knowledge like a rules-based approach (e.g., [49]) or further refinement or subjectivity as is typical for visual interpretation [54,55]. Similarly, it does not rely on the identification of any specific landscape features, such as the dune crest, which can vary depending on the dataset and extraction technique used [19,56]. Furthermore, the DEM-derived metrics are not seasonally dependent, as compared to imagery-based metrics (NDVI and EVI), thus reducing biases related to data collection timing [57,58].

Habitat classifications were constrained to those of the training dataset, and the results highlight areas of improvement for future model development. The model currently does not differentiate between vegetation habitats in different geomorphic zones (i.e., upland grasses and salt marsh species are grouped as herbaceous), potentially overgeneralizing the results. Different sub-classifications have been applied to other models but doing so does not necessarily improve accuracy [46,55]. For example, Enwright et al. partitioned the dune habitat into multiple sub-classifications but had greater accuracy grouping these into one overarching 'dune' class [55]. Additionally, factors that influence vegetation growth, such as hydrology, sediment transport, or episodic events, were not explicitly incorporated into this model and can affect vegetation distributions [43,59]. It is important to note that this example does not consider submerged habitats (i.e., seagrass beds) due to limitations in collecting lidar in the turbid, shallow nearshore environment [60] as well as lack of available submerged habitat data in the area.

Habitat distribution maps can play an essential intermediary step towards justifying conservation and planning efforts. Conservation efforts, especially publicly funded ones, often must be justified with societal benefits [61]. The nitrogen sequestration results can be used to distinguish current and potential future habitat boundaries of herbaceous and woody habitat transitions affected by climate change in barrier islands [40,42,62–64]. As habitat boundaries change, these often nutrient-limited systems may experience substantial increases in both N and C storage resulting from high litterfall in woody habitats (e.g., shrub thickets) [63]. Our current results integrate the impact of both vegetation type and elevation on these storage processes. Identifying change in C and N sequestration at a local scale allows for further understanding of the role of barrier island systems in C and N stocks and fluxes at regional and global scales. However, it may be more appropriate to interpret the nutrient sequestration rates as an order-of-magnitude calculation rather than an exact value because the model results assume the entire cell (25 m^2) was fully vegetated and under-predicted woody vegetation and over-predicted herbaceous vegetation, which have different nutrient concentrations.

Depending on how back-barrier habitat develops and maintains in the face of sea-level rise, barrier islands, such as Assateague, may serve as an important carbon sink, or a net source [65]. Because barrier island habitats can store carbon, which has been well documented in salt marsh habitats [66,67], any efforts to conserve, restore, or build vegetated habitat can impact carbon dynamics and can be monetarily justified. Carbon stored can be converted to dollars per m^2 after habitat cover and sequestration calculations are made, such as in the application presented here. The direct assignment of a monetary valuation provides an economic justification regarding different actions affecting habitat loss or gain [29,65,68,69]. Further, using broader habitat classifications in these estimations (e.g., herbaceous versus woody compared to distinguishing between dunes, marsh, grassland among herbaceous) helps demonstrate the interconnectedness among barrier island habitats and potentially to raise public awareness of their ecosystem services [29,66].

6. Conclusions

The model developed for this study utilized DEM-derived metrics (elevation change, slope, and distance to shore) to predict sparse, herbaceous, and woody habitats across a barrier island landscape. It is a relatively simple, but effective tool requiring no prior system knowledge to run and output results. The habitat maps produced can be used for a variety of purposes. Uses may include, but are not limited to, coupling with hydrodynamic models to better represent ecogeomorphic feedbacks over time, predicting habitat change

over time, and estimating ecosystem service values. Landscape classification models are a first step towards predicting changing species and habitat distributions and linking those changes to patterns and processes with cause-and-effect relationships, providing insight into barrier island resilience for coastal managers.

Supplementary Materials: The following are available online at https://www.mdpi.com/article/10.3390/rs14061377/s1, Figure S1: 2012 habitat observations (A), habitat predictions using the equations from Table 4 (B), and model accuracy assessment (C) in which observations were compared to predictions. The legend is in order of habitat confusions that are assumed to be more likely (i.e., Herbaceous:Woody confusions) to habitats confusions that are assumed to be less likely (Woody:Sparse confusions).

Author Contributions: Conceptualization, S.A., M.K.R. and T.M.S.; formal analysis, E.R.R.; funding acquisition, S.A., M.K.R. and T.M.S.; investigation, E.R.R.; methodology, S.A., M.K.R. and T.M.S.; project administration, E.R.R. and T.M.S.; software, E.R.R.; supervision, S.A. and M.K.R.; validation, E.R.R.; visualization, E.R.R.; writing—original draft, E.R.R., B.R.C. and S.A.; writing—review and editing, E.R.R., B.R.C., S.A., M.K.R. and T.M.S. All authors have read and agreed to the published version of the manuscript.

Funding: This research was funded by the US Army Corps of Engineers Navigation Systems and Aquatic Nuisance Species Research Programs.

Institutional Review Board Statement: Not applicable.

Informed Consent Statement: Not applicable.

Data Availability Statement: No new data were created or analyzed in this study. Data sharing is not applicable to this article.

Conflicts of Interest: The authors declare no conflict of interest.

References

1. Luisetti, T.; Turner, R.K.; Jickells, T.; Andrews, J.; Elliott, M.; Schaafsma, M.; Beaumont, N.; Malcolm, S.; Burdon, D.; Adams, C.; et al. Coastal Zone Ecosystem Services: From science to values and decision making; a case study. *Sci. Total Environ.* **2014**, *493*, 682–693. [CrossRef] [PubMed]
2. Arkema, K.K.; Guannel, G.; Verutes, G.; Wood, S.A.; Guerry, A.; Ruckelshaus, M.; Kareiva, P.; Lacayo, M.; Silver, J.M. Coastal habitats shield people and property from sea-level rise and storms. *Nat. Clim. Chang.* **2013**, *3*, 913–918. [CrossRef]
3. IPCC. *Climate Change 2014: Synthesis Report. Contribution of Working Groups I, II and III to the Fifth Assessment Report of the Intergovernmental Panel on Climate Change*; Core Writing Team, Pachauri, R.K., Meyer, L.A., Eds.; IPCC: Geneva, Switzerland, 2014; p. 151.
4. Altman, S.; Reif, M.K.; Swannack, T.M. *Linking Critical Ecological Processes to Landscape Pattern: Implications for USACE Planning and Operations*; ERDC/CHL CHETN-V-23; US Army Engineer Research and Development Center: Vicksburg, MS, USA, 2014; p. 9.
5. Reif, M.K.; Swannack, T.M. *Development of Landscape Metrics to Support Process-Driven Ecological Modeling*; ERDC/EL TR-14-6; US Army Engineer Research and Development Center: Vicksburg, MS, USA, 2014; p. 38.
6. Spalding, M.D.; Ruffo, S.; Lacambra, C.; Meliane, I.; Hale, L.Z.; Shepard, C.C.; Beck, M.W. The role of ecosystems in coastal protection: Adapting to climate change and coastal hazards. *Ocean Coast. Manag.* **2014**, *90*, 50–57. [CrossRef]
7. Stallins, J.A.; Parker, A.J. The Influence of Complex Systems Interactions on Barrier Island Dune Vegetation Pattern and Process. *Ann. Assoc. Am. Geogr.* **2003**, *93*, 13–29. [CrossRef]
8. Feagin, R.A.; Figlus, J.; Zinnert, J.C.; Sigren, J.; Martínez, M.L.; Silva, R.; Smith, W.K.; Cox, D.; Young, D.R.; Carter, G. Going with the flow or against the grain? The promise of vegetation for protecting beaches, dunes, and barrier islands from erosion. *Front. Ecol. Environ.* **2015**, *13*, 203–210. [CrossRef]
9. Guisan, A.; Thuiller, W. Predicting species distribution: Offering more than simple habitat models. *Ecol. Lett.* **2005**, *8*, 993–1009. [CrossRef] [PubMed]
10. Wiersma, Y.F.; Huettmann, F.; Drew, C.A. Introduction: Landscape modeling of species and their habitats: History, uncertainty, and complexity. In *Predictive Species and Habitat Modeling in Landscape Ecology: Concepts and Applications*; Springer: New York, NY, USA, 2011; pp. 1–6. ISBN 9781441973894.
11. Hladik, C.; Alber, M. Classification of salt marsh vegetation using edaphic and remote sensing-derived variables. *Estuar. Coast. Shelf Sci.* **2014**, *141*, 47–57. [CrossRef]
12. Dunkin, L.; Reif, M.; Altman, S.; Swannack, T. A Spatially Explicit, Multi-Criteria Decision Support Model for Loggerhead Sea Turtle Nesting Habitat Suitability: A Remote Sensing-Based Approach. *Remote Sens.* **2016**, *8*, 573. [CrossRef]

13. Hood, W.G. Landscape allometry and prediction in estuarine ecology: Linking landform scaling to ecological patterns and processes. *Estuaries Coasts* **2007**, *30*, 895–900. [CrossRef]
14. Hacker, S.D.; Jay, K.R.; Cohn, N.; Goldstein, E.B.; Hovenga, P.A.; Itzkin, M.; Moore, L.J.; Mostow, R.S.; Mullins, E.V.; Ruggiero, P. Species-specific functional morphology of four US atlantic coast dune grasses: Biogeographic implications for dune shape and coastal protection. *Diversity* **2019**, *11*, 82. [CrossRef]
15. Charbonneau, B.R.; Dohner, S.M.; Wnek, J.P.; Barber, D.; Zarnetske, P.; Casper, B.B. Vegetation effects on coastal foredune initiation: Wind tunnel experiments and field validation for three dune-building plants. *Geomorphology* **2021**, *378*, 107594. [CrossRef]
16. Miller, D.L.; Thetford, M.; Schneider, M. Distance from the Gulf Influences Survival and Growth of Three Barrier Island Dune Plants. *J. Coast. Res.* **2008**, *4*, 261–266. [CrossRef]
17. Shao, G.; Shugart, H.H.; Hayden, B.P. Functional classifications of coastal barrier island vegetation. *J. Veg. Sci.* **1996**, *7*, 391–396. [CrossRef]
18. Young, D.R.; Brantley, S.T.; Zinnert, J.C.; Vick, J.K. Landscape position and habitat polygons in a dynamic coastal environment. *Ecosphere* **2011**, *2*, art71. [CrossRef]
19. Wernette, P.; Houser, C.; Bishop, M.P. An automated approach for extracting Barrier Island morphology from digital elevation models. *Geomorphology* **2016**, *262*, 1–7. [CrossRef]
20. Enwright, N.M.; Wang, L.; Wang, H.; Osland, M.J.; Feher, L.C.; Borchert, S.M.; Day, R.H. Modeling Barrier Island Habitats Using Landscape Position Information. *Remote Sens.* **2019**, *11*, 976. [CrossRef]
21. Brock, J.C.; Purkis, S.J. The emerging role of lidar remote sensing in coastal research and resource management. *J. Coast. Res.* **2009**, *25*, 1–5. [CrossRef]
22. Gesch, D.B. Analysis of lidar elevation data for improved identification and delineation of lands vulnerable to sea-level rise. *J. Coast. Res.* **2009**, *25*, 49–58. [CrossRef]
23. Stockdon, H.F.; Sallenger, A.H.; Holman, R.A.; Howd, P.A. A simple model for the spatially-variable coastal response to hurricanes. *Mar. Geol.* **2007**, *238*, 1–20. [CrossRef]
24. Lopes, C.L.; Mendes, R.; Caçador, I.; Dias, J.M. Assessing salt marsh loss and degradation by combining long-term LANDSAT imagery and numerical modelling. *L. Degrad. Dev.* **2021**, *32*, 4534–4545. [CrossRef]
25. McCarthy, M.J.; Halls, J.N. Habitat mapping and change assessment of coastal environments: An examination of worldview-2, quickbird, and ikonos satellite imagery and airborne lidar for mapping barrier island habitats. *ISPRS Int. J. Geo-Inf.* **2014**, *3*, 297–325. [CrossRef]
26. Valentini, E.; Taramelli, A.; Cappucci, S.; Filipponi, F.; Xuan, A.N. Exploring the dunes: The correlations between vegetation cover pattern and morphology for sediment retention assessment using airborne multisensor acquisition. *Remote Sens.* **2020**, *12*, 1229. [CrossRef]
27. Malthus, T.J.; Mumby, P.J. Remote sensing of the coastal zone: An overview and priorities for future research. *Int. J. Remote Sens.* **2003**, *24*, 2805–2815. [CrossRef]
28. Sneddon, L.; Menke, J.; Berdine, A.; Largay, E.; Gawler, S. Vegetation classification and mapping of Assateague Island National Seashore. In *Natural Resource Report NPS/ASIS/NRR—2017/1422*; National Park Service: Fort Collins, CO, USA, 2017; pp. 1–119.
29. Rossi, A.M.; Rabenhorst, M.C. Organic carbon dynamics in soils of Mid-Atlantic barrier island landscapes. *Geoderma* **2019**, *337*, 1278–1290. [CrossRef]
30. Schupp, C.A.; Winn, N.T.; Pearl, T.L.; Kumer, J.P.; Carruthers, T.J.B.; Zimmerman, C.S. Restoration of overwash processes creates piping plover (Charadrius melodus) habitat on a barrier island (Assateague Island, Maryland). *Estuar. Coast. Shelf Sci.* **2013**, *116*, 11–20. [CrossRef]
31. U.S. Army Corps of Engineers. *Ocean City, Maryland and Vicinity Water Resources Study: Final Integrated Feasibility Report and Environmental Impact Statement*; U.S. Army Corps of Engineers: Baltimore, MD, USA, 1998.
32. Schupp, C.A.; Bass, G.P.; Grosskopf, W.G. Sand bypassing restores natural processes to Assateague Island, Maryland. In Proceedings of the Sixth International Symposium on Coastal Engineering and Science of Coastal Sediment Process, New Orleans, Louisiana, 13–17 May 2007. [CrossRef]
33. Carruthers, T.J.B.; Beckert, K.; Schupp, C.A.; Saxby, T.; Kumer, J.P.; Thomas, J.; Sturgis, B.; Dennison, W.C.; Williams, M.; Fisher, T.; et al. Improving management of a mid-Atlantic coastal barrier island through assessment of habitat condition. *Estuar. Coast. Shelf Sci.* **2013**, *116*, 74–86. [CrossRef]
34. Roman, C.T.; Nordstrom, K.F. The effect of erosion rate on vegetation patterns of an east coast barrier island. *Estuar. Coast. Shelf Sci.* **1988**, *26*, 233–242. [CrossRef]
35. OCM: Office for Coastal Management. 2000 Fall East Coast NOAA/USGS/NASA Airborne LiDAR Assessment of Coastal Erosion (ALACE) Project for the US Coastline. Available online: https://www.fisheries.noaa.gov/inport/item/48163 (accessed on 1 June 2021).
36. OCM. USACE Post Sandy Topographic LiDAR: Virginia and Maryland. 2012. Available online: https://www.fisheries.noaa.gov/inport/item/49610 (accessed on 1 June 2021).
37. Pedregosa, F.; Varoquaux, G.; Gramfort, A.; Michel, V.; Thirion, B.; Grisel, O.; Blondel, M.; Prettenhofer, P.; Weiss, R.; Dubourg, V. Scikit-learn: Machine learning in Python. *J. Mach. Learn. Res.* **2011**, *12*, 2825–2830.
38. Cohen, J. A Coefficient of Agreement for Nominal Scales. *Educ. Psychol. Meas.* **1960**, *20*, 37–46. [CrossRef]

39. Allouche, O.; Tsoar, A.; Kadmon, R. Assessing the accuracy of species distribution models: Prevalence, kappa and the true skill statistic (TSS). *J. Appl. Ecol.* **2006**, *43*, 1223–1232. [CrossRef]
40. Rossi, A.M. Pedogenesis and Hydrogeomorphology of Soils in Mid-Atlantic Barrier Island Landscapes. Doctoral Dissertation, University of Maryland, College Park, MD, USA, 2014.
41. Landis, J.R.; Koch, G.G. The Measurement of Observer Agreement for Categorical Data. *Biometrics* **1977**, *33*, 159. [CrossRef] [PubMed]
42. Zinnert, J.C.; Stallins, J.A.; Brantley, S.T.; Young, D.R. Crossing scales: The complexity of barrier-island processes for predicting future change. *Bioscience* **2017**, *67*, 39–52. [CrossRef]
43. Brantley, S.T.; Bissett, S.N.; Young, D.R.; Wolner, C.W.V.; Moore, L.J. Barrier island morphology and sediment characteristics affect the recovery of dune building grasses following storm-induced overwash. *PLoS ONE* **2014**, *9*, e104747. [CrossRef] [PubMed]
44. Nardin, W.; Larsen, L.; Fagherazzi, S.; Wiberg, P. Tradeoffs among hydrodynamics, sediment fluxes and vegetation community in the Virginia Coast Reserve, USA. *Estuar. Coast. Shelf Sci.* **2018**, *210*, 98–108. [CrossRef]
45. Zinnert, J.C.; Shiflett, S.A.; Via, S.; Bissett, S.; Dows, B.; Manley, P.; Young, D.R. Spatial–Temporal Dynamics in Barrier Island Upland Vegetation: The Overlooked Coastal Landscape. *Ecosystems* **2016**, *19*, 685–697. [CrossRef]
46. Zeigler, S.L.; Sturdivant, E.J.; Gutierrez, B.T. *Evaluating Barrier Island Characteristics and Piping Plover (Charadrius Melodus) Habitat Availability along the U.S. Atlantic Coast—Geospatial Approaches and Methodology*; Open-File Report 2019–1071; U.S. Geological Survey: Reston, VA, USA, 2019; p. 34.
47. Houser, C.; Hapke, C.; Hamilton, S. Controls on coastal dune morphology, shoreline erosion and barrier island response to extreme storms. *Geomorphology* **2008**, *100*, 223–240. [CrossRef]
48. Small-Lorenz, S.L.; Shadel, W.P.; Glick, P. *Building Ecological Solutions to Coastal Community Hazards*; The National Wildlife Federation: Washington, DC, USA, 2017; p. 95.
49. Halls, J.N.; Frishman, M.A.; Hawkes, A.D. An automated model to classify barrier island geomorphology using lidar data and change analysis (1998–2014). *Remote Sens.* **2018**, *10*, 1109. [CrossRef]
50. Hayden, B.P.; Santos, M.C.F.V.; Shao, G.; Kochel, R.C. Geomorphological controls on coastal vegetation at the Virginia Coast Reserve. *Geomorphology* **1995**, *13*, 283–300. [CrossRef]
51. Young, D.R.; Porter, J.H.; Bachmann, C.M.; Shao, G.; Fusina, R.A.; Bowles, J.H.; Korwan, D.; Donato, T.F. Cross-scale patterns in shrub thicket dynamics in the Virginia barrier complex. *Ecosystems* **2007**, *10*, 854–863. [CrossRef]
52. Young, D.R.; Shao, G.; Porter, J.H. Spatial and temporal growth dynamics of barrier island shrub thickets. *Am. J. Bot.* **1995**, *82*, 638–645. [CrossRef]
53. Doyle, T.B.; Woodroffe, C.D. The application of LiDAR to investigate foredune morphology and vegetation. *Geomorphology* **2018**, *303*, 106–121. [CrossRef]
54. Ray, N.; Burgman, M.A. Subjective uncertainties in habitat suitability maps. *Ecol. Modell.* **2006**, *195*, 172–186. [CrossRef]
55. Enwright, N.M.; Wang, L.; Borchert, S.M.; Day, R.H.; Feher, L.C.; Osland, M.J. Advancing barrier island habitat mapping using landscape position information. *Prog. Phys. Geogr. Earth Environ.* **2019**, *43*, 425–450. [CrossRef]
56. Houser, C.; Bishop, M.; Wernette, P. Short communication: Multi-scale topographic anisotropy patterns on a Barrier Island. *Geomorphology* **2017**, *297*, 153–158. [CrossRef]
57. Feilhauer, H.; Thonfeld, F.; Faude, U.; He, K.S.; Rocchini, D.; Schmidtlein, S. Assessing floristic composition with multispectral sensors-A comparison based: On monotemporal and multiseasonal field spectra. *Int. J. Appl. Earth Obs. Geoinf.* **2012**, *21*, 218–229. [CrossRef]
58. García-Romero, L.; Hernández-Cordero, A.I.; Hernández-Calvento, L.; Espino, E.P.-C.; López-Valcarcel, B.G. Procedure to automate the classification and mapping of the vegetation density in arid aeolian sedimentary systems. *Prog. Phys. Geogr. Earth Environ.* **2018**, *42*, 330–351. [CrossRef]
59. Aguilar, C.; Zinnert, J.C.; Polo, M.J.; Young, D.R. NDVI as an indicator for changes in water availability to woody vegetation. *Ecol. Indic.* **2012**, *23*, 290–300. [CrossRef]
60. Klemas, V. Beach profiling and LIDAR bathymetry: An overview with case studies. *J. Coast. Res.* **2011**, *27*, 1019–1028. [CrossRef]
61. Chan, K.M.A.; Pringle, R.M.; Ranganathan, J.; Boggs, C.L.; Chan, Y.L.; Ehrlich, P.R.; Haff, P.K.; Heller, N.E.; Al-Khafaji, K.; Macmynowski, D.P. When Agendas Collide: Human Welfare and Biological Conservation. *Conserv. Biol.* **2007**, *21*, 59–68. [CrossRef] [PubMed]
62. Brantley, S.T.; Young, D.R. Shifts in litterfall and dominant nitrogen sources after expansion of shrub thickets. *Oecologia* **2008**, *155*, 337–345. [CrossRef] [PubMed]
63. Brantley, S.T.; Young, D.R. Shrub expansion stimulates soil C and N storage along a coastal soil chronosequence. *Glob. Chang. Biol.* **2010**, *16*, 2052–2061. [CrossRef]
64. Huang, H.; Zinnert, J.C.; Wood, L.K.; Young, D.R.; D'Odorico, P. Non-linear shift from grassland to shrubland in temperate barrier islands. *Ecology* **2018**, *99*, 1671–1681. [CrossRef] [PubMed]
65. Theuerkauf, E.J.; Rodriguez, A.B. Placing barrier-island transgression in a blue-carbon context. *Earth's Futur.* **2017**, *5*, 789–810. [CrossRef]
66. Duarte, C.M.; Dennison, W.C.; Orth, R.J.W.; Carruthers, T.J.B. The Charisma of Coastal Ecosystems: Addressing the Imbalance. *Estuaries Coasts* **2008**, *31*, 233–238. [CrossRef]

67. Duarte, C.M.; Losada, I.J.; Hendriks, I.E.; Mazarrasa, I.; Marbà, N. The role of coastal plant communities for climate change mitigation and adaptation. *Nat. Clim. Chang.* **2013**, *3*, 961–968. [CrossRef]
68. Beaumont, N.J.; Jones, L.; Garbutt, A.; Hansom, J.D.; Toberman, M. The value of carbon sequestration and storage in coastal habitats. *Estuar. Coast. Shelf Sci.* **2014**, *137*, 32–40. [CrossRef]
69. Drius, M.; Carranza, M.L.; Stanisci, A.; Jones, L. The role of Italian coastal dunes as carbon sinks and diversity sources. A multi-service perspective. *Appl. Geogr.* **2016**, *75*, 127–136. [CrossRef]